PHYSICAL REVIEW D **81,** 064001 (2010)

Perturbations of black p-branes

Elcio Abdalla*
Instituto de Física, Universidade de São Paulo, CP 66318, 05315-970, São Paulo-SP, Brazil

Owen Pavel Fernandez Piedra†
Departamento de Física y Química, Facultad de Mecánica, Universidad de Cienfuegos, Carretera a Rodas, km 4, Cuatro Caminos, Cienfuegos, Cuba

Jeferson de Oliveira‡
Instituto de Física, Universidade de São Paulo, CP 66318, 05315-970, São Paulo-SP, Brazil

C. Molina§
Escola de Artes, Ciências e Humanidades, Universidade de São Paulo Av. Arlindo Bettio 1000, CEP 03828-000, São Paulo-SP, Brazil
(Received 7 December 2009; published 2 March 2010)

We consider black p-brane solutions of the low-energy string action, computing scalar perturbations. Using standard methods, we derive the wave equations obeyed by the perturbations and treat them analytically and numerically. We have found that tensorial perturbations obtained via a gauge-invariant formalism leads to the same results as scalar perturbations. No instability has been found. Asymptotically, these solutions typically reduce to a $\mathrm{AdS}_{(p+2)} \times S^{(8-p)}$ space which, in the framework of Maldacena's conjecture, can be regarded as a gravitational dual to a conformal field theory defined in a $(p+1)$-dimensional flat space-time. The results presented open the possibility of a better understanding the AdS/CFT correspondence, as originally formulated in terms of the relation among brane structures and gauge theories.

DOI: 10.1103/PhysRevD.81.064001 PACS numbers: 04.50.Gh, 04.70.Bw, 04.30.Nk

I. INTRODUCTION

String theory and the subsequent idea of branes have been, in recent years, the almost standard theory describing the physics of quantum space-time, especially near the big bang or even before it [1]. The discovery of the relation between anti–de Sitter (AdS) space physics and conformal field theories (CFT) on the boundary of that space, the so-called AdS/CFT correspondence [2,3] implied further interest in the structure of the string-membrane theory.

The p-brane extended solutions are considered fundamental in the understanding of the nonperturbative string theory regime. They interpolate $\mathrm{AdS}_{p+2} \times S^{d-p-2}$ and d-dimensional Minkowski space-time [4]. This connection was important for the conjecture presented by Maldacena in 1997 [2], which opened the way for the gravitation-field theory dualities. In this context, a better understanding of the perturbative dynamics of the p-brane solutions are relevant for the structural aspects of the AdS/CFT correspondence and its latter extensions. Such extensions can provide new hints about Yang-Mills theory with special interest in what concerns the difficult question of a quark gluon plasma; see for instance [5–7]. Besides, in the framework of AdS/CFT correspondence it is possible to study the glueball mass spectrum analyzing the dynamics of a scalar field in the near horizon limit of the black p-brane solutions [8–10]. The poles of the retarded function of the simplest glueball state, generated by the operator $\mathcal{O} = \mathrm{Tr}(F^2)$, are the quasinormal modes of the dual AdS black hole in the corresponding near horizon limit.

A fundamental feature of the p-brane backgrounds is the possible existence of event horizons. In this sense, they may be viewed as generalizations of the usual four-dimensional black holes. Perturbations of black hole solutions are well known [11,12] and several numerical methods exist, being under full control to handle the information gathered from such perturbations [13–15].

We intend here to first define a perturbation of a p-brane solution using standard separation of variables and subsequently treat, analytically and numerically, the wave equation for the scalar perturbation. The employed methods are largely independent, aiming to a cross-check of the results. We also consider gauge-invariant gravitational perturbations. The results turn out to be exactly the same as scalar case.

One very recent work complements our analysis presented here [16]. But although the presented work and [16] are complementary and relevant in terms of the AdS/CFT correspondence, they treat different geometries and focus on different issues. The results presented in this paper address directly the role of the brane structure (in the sense presented in [2,4]) on the gravitation-field theory duality, specifically searching for possible instabilities.

*eabdalla@fma.if.usp.br
†opavel@ucf.edu.cu
‡jeferson@fma.if.usp.br
§cmolina@usp.br

The paper is organized as follows. Section II provides reviews of p-brane background considered in this work. In Sec. III, the perturbative dynamics is formulated and developed, followed by Secs. IV and V where the nonextreme and extremal scenarios are specifically treated. In Sec. VI some final comments are presented.

II. p-BRANE SOLUTIONS

Solutions of ten dimensional supergravity describing the so-called p-branes are well known. Let us consider the bosonic sector of type II supergravity in ten dimensions, given by [3,17]

$$S = \frac{1}{(2\pi)^7 (l_s)^8} \int dx^{10} \sqrt{-g} \bigg[e^{-2\phi}(R + 4(\nabla\phi)^2) - \frac{2}{(8-p)!} F^2_{p+2} \bigg], \tag{1}$$

where l_s is the string length, g the determinant of the metric tensor g_{ab}, R the Ricci scalar, ϕ the dilaton field, and F_{p+2} the field strength of the potential A_{p+1}.

The solution of Einstein's equations with N electric charges and p dimensions is obtained from the ansatz [17]

$$ds^2 = ds^2_{10-p} + e^{\alpha} \sum_{i=1}^{p} dy^i dy^i, \tag{2}$$

where ds^2_{10-p} is the line element with Lorentzian signature in $(10-p)$ dimensions, α is a function of x, that is the bulk's radial coordinate, and the meaning of N as a charge arises from the Gauss law. We can write a full solution as

$$ds^2 = -A(x)dt^2 + B(x)[dr^2 + r^2 d\Omega^2_{p-1}] + C(x)dx^2 + x^2 D(x) d\Omega^2_{8-p}, \tag{3}$$

where $A(x) = (1-(a/x)^{7-p})(1-(b/x)^{7-p})^{-1/2}$, $C(x) = (1-(b/x)^{7-p})^{\alpha_1}(1-(a/x)^{7-p})^{-1}$, $B(x) = \sqrt{1-(b/x)^{7-p}}$, $D(x) = (1-(b/x)^{7-p})^{\alpha_2}$, with $\alpha_1 = -\frac{1}{2} - \frac{(5-p)}{(7-p)}$ and $\alpha_2 = \frac{1}{2} - \frac{(5-p)}{(7-p)}$. The mass per unit volume is $M = \frac{1}{(7-p)\kappa_1}[(8-p)a^{7-p} - b^{7-p}]$, the electric charge $N = \frac{1}{\kappa_2}[ab]^{(7-p)/2}$, $\kappa_1 = (2\pi)^7 d_p l_p^8$, $\kappa_2 = d_p g_s l_s^{7-p}$, and g_s is the string coupling, l_p the Planck length in ten dimensions, and $d_p = 2^{5-p}\pi^{(5-p)/2}\Gamma((7-p)/2)$. Absence of naked singularities implies

$$M \geq \frac{N}{(2\pi)^p g_s l_s^{p+1}}. \tag{4}$$

Considering the nonextreme scenario, the maximal extension of the metric describes a black brane geometry, with an event horizon located at $x = a$. If $p \neq 3$, a curvature singularity is present at $x = b$, while if $p = 3$ we observe that, in addition to the outer horizon at $x = a$, there is also an inner horizon at $x = b$, with the singularity at $x = 0$. That behavior is observed in the Kretschmann scalar $\mathcal{K}_p(x) = R_{abcd}R^{abcd}$, where R_{abcd} are the components of the Riemann tensor, as seen in the expression for the divergent term

$$\mathcal{K}_p(x) \sim \frac{1}{(1-(\frac{b}{x})^{7-p})^{\delta(p)} x^{2(9-p)}}, \tag{5}$$

where $\delta(p) = \frac{1}{7-p}[(1+p) + 2(5-p)]$ if p is even, and $\delta(p) = \frac{30p}{40}(p-1)(p-3) - \frac{p}{6}(p-1)(p-5) + \frac{8p}{35}(p-3)(p-5)$ if p is odd.

For extremal p-branes the metric reads

$$ds^2 = E(x)[-dt^2 + dr^2 + r^2 d\Omega^2_{p-1}] + F(x)dx^2 + x^2 G(x) d\Omega^2_{8-p}, \tag{6}$$

where $E(x) = \sqrt{1-(a/x)^{7-p}}$, $F(x) = (1-(a/x)^{7-p})^{\gamma_1}$, $G(x) = (1-(a/x)^{7-p})^{\alpha_2}$, $\gamma_1 = \alpha_1 - 1$.

In the extreme case, the curvature singularity is located at $r = a$ and the metric does not have an extension if $p \neq 3$. We have a curvature singularity, but its structure depends on the value of p. If $p = 6$ the singularity is timelike, and the proper definition of a Cauchy problem is delicate. On the other hand, if $p = 0, 1, 2, 5$, the singularity ($r = a$) is null [3], and therefore much milder. In spite of the absence of an event horizon, the manifold is globally hyperbolic, and the wave problem is well-posed. For the extreme case and $p = 3$, there is an analytic continuation of the metric beyond $r = a$ and we have again a black hole solution as pointed out in [3].

III. SCALAR AND GRAVITATIONAL PERTURBATIVE DYNAMICS

We initially consider a massless scalar field in the background of our 10-dimensional solution. We will show in the following that this scenario is more general. This perturbation is described by the Klein-Gordon equation

$$\Delta_{10}\Phi \equiv [\Delta_p(r, \theta_{(p-1)}) + \Delta_{10-p}(t, x, \lambda_{(8-p)})]\Phi = 0, \tag{7}$$

where the first term refers to the subspace $dr^2 + r^2 d\Omega^2_{p-1}$ and the second to the bulk coordinates $(t, x, \lambda_{(8-p)})$. We denote the angular coordinates in $d\Omega^2_{p-1}$ and $d\Omega^2_{8-p}$ respectively by $\theta_{(p-1)}$ and λ_{8-p}.

Such equation can be separated by the ansatz $\Phi(x^A) = \sum_{l,m} R_l(r) Y_{lm}(\theta_i) \sum_{L,q} \Psi_L(t,x) Y_{Lq}(\lambda_j)$, where $Y_{lm}(\theta_i)$ and $Y_{Lq}(\lambda_j)$ are the well-known spherical harmonics in $(p-1)$ and $(8-p)$ dimensions respectively [18], resulting in the differential equations

$$\frac{1}{r^{(p-1)}} \frac{d}{dr}\left(r^{(p-1)} \frac{dR_l}{dr}\right) + \left[\beta^2 - \frac{l(l+p-2)}{r^2}\right] R_l = 0, \tag{8}$$

$$-\frac{\partial^2 \Psi_L}{\partial t^2} + \frac{1}{A(x)} \Delta_x \Psi_L + u(x)\Psi_L = 0, \tag{9}$$

where $u(x) = -\frac{A(x)}{B(x)}[\beta^2 + \frac{B(x)}{x^2 D(x)} L(L+7-p)]$. Moreover, β is a constant arising from the brane $\{r, \theta_{(p-1)}\}$ and bulk $\{t, x, \lambda_{(8-p)}\}$ variables separation. The differential operator Δ_x is given by

$$\Delta_x = \frac{\frac{\partial}{\partial x}(\sqrt{A(x)B(x)C(x)D^{(8-p)}}x^{8-p}\frac{\partial}{\partial x})}{\sqrt{A(x)B(x)C(x)D^{(8-p)}}x^{8-p}}. \quad (10)$$

The solution of Eq. (8) is $R_l(r) = A_1 r^{1-p/2} J_\gamma(\beta r) + A_2 r^{1-p/2} Y_\gamma(\beta r)$, with $\gamma = \frac{1}{2} \times \sqrt{p^2 - 4p + 4 + 4l(l+p-2)}$, A_1 and A_2 being constants, $J_\gamma(\beta r)$ and $Y_\gamma(\beta r)$ the Bessel functions. Finiteness at origin implies $A_2 = 0$ and $R_l(r) = A_1 r^{1-p/2} J_\gamma(\beta r)$. Therefore, β has a continuous spectrum of allowed values, and we notice in (9) that its square acts as a mass for the Klein-Gordon field. Performing the same analysis for a time-independent scalar field in the near horizon limit of the metric (3), the β^2 parameter can be interpreted as the glueball mass.

A "time-independent approach" can be explored expanding the function $\Psi_L(t, x)$ with a Laplace-like transform [19]. Within this approach, we obtain the equation

$$\frac{d^2}{dr_*^2} Z_L + [k^2 - V(x)] Z_L = 0, \quad (11)$$

where we defined the tortoise coordinate as $dr_*/dx = \sqrt{C(x)/A(x)}$, $\Psi_L(t, x) = \int e^{i\omega t} b(x) Z_L(x) d\omega$ with $b(x) = \frac{1}{x^{(8-p)/2} B(x)^{p/4} D(x)^{(8-p)/4}}$, $k^2 = \omega^2 - \beta^2$ and the effective potential is given by the expression

$$V(x) = \left[\frac{A(x)}{B(x)} - 1\right]\beta^2 + \frac{A(x)}{x^2 D(x)} L(L+7-p) - \frac{1}{b(x)}[h(x)b(x)'' - g(x)b(x)'], \quad (12)$$

where the primes denotes differentiation with respect to x, $h(x) = A(x)/C(x)$, and $g(x) = \frac{A(x)}{C(x)} \frac{d}{dx}\{\ln[\frac{A(x)B(x)(D(x)x)^{8-p}}{C(x)}]\}$.

We can also consider the problem of the linear perturbations using the gauge-invariant formalism proposed by Ishibashi *et al.* [12]. In this formalism we expand the gravitational perturbations in terms of tensor harmonics Π_{ij}, and perturbations of Einstein equations are expressed as a group of equations for gauge-invariant quantities. Such quantities are grouped in three types: tensor, vector, and scalar. For the sake of simplicity, we only consider in the following the tensor sector of gravitational perturbations. The space-time is considered as describing an $m + n$-dimensional manifold $\mathcal{M}$, which is locally written as the warped product $g_{\alpha\beta} dz^\alpha dz^\beta = g_{ab}(y) dy^a dy^b + f(y)\gamma_{ij} dx^i dx^j$, where $\gamma_{ij}(y)$ is the metric of an n-dimensional maximally symmetric space of constant spatial curvature, and $g_{ab}(y)$ the metric of an arbitrary m-dimensional space-time.

Following Ref. [12] the following equation for the gauge-invariant quantity H_T can be obtained:

$$\Box H_T + \frac{8-p}{f} Dr \cdot DH_T - \frac{l(l+7-p)}{f^2} H_T = 0, \quad (13)$$

where $\Box$ is the d'Alembert operator written on the metric $g_{ab}(y)$. Introducing in the above equation the master variable $\Phi = f^{(8-p)/2} H_T$ we found the same result that we have already obtained from the scalar Klein-Gordon equation.

At this point it is appropriate to make the following important observation: the spectrum of quasinormal frequencies for the scalar field perturbations contains extra modes with respect to the tensor perturbations, because the modes for the last case only appear for multipole numbers equal to or greater than 2. Thus, for the black p-brane, we need only to consider a test scalar field perturbation. Extracting the $l \geq 2$ terms for the obtained spectrum of scalar quasinormal frequencies, we obtain the spectrum for the tensor gravitational perturbations.

IV. NONEXTREME CASE

The effective potentials derived above determine the perturbative dynamics. Of particular importance for this dynamics are the quasinormal modes. They are defined as solutions of the wave equations which satisfy the in-going and out-going boundary conditions. These modes are particularly relevant in the intermediate time behavior of the perturbation.

With arbitrary L, two different and independent numerical tools will be used in this work to calculate the quasinormal frequencies: a "frequency domain" approach based on a sixth order WKB technique [20], and a "time domain" method based on a numerical characteristic integration scheme [21–23]. Both algorithms are well established.

The WKB expressions are usually accurate and straightforward. But the approach is not generally applicable. For instance, in Fig. 1 the effective potential is presented for a few values of β with $p = 3, 6$. We observe that the maximum of the effective potential decreases as β increases for a given p. For a sufficiently large value of β the potential becomes negative. This behavior appears explicitly for $p = 6$ with $\beta = 1$. Therefore, we cannot obtain the quasinormal frequencies for all values of p and β using the WKB formula. The instability for effective potentials that exhibit a negative gap is not excluded [24,25]. Direct time integration can be used for such scenarios. *We have found no instabilities after an extensive exploration with* $\beta^2 \geq 0$.

Within the "time-domain" approach, we have observed the usual picture in the perturbative dynamics. After the initial transient regime, the quasinormal mode phase follows as well as a late-time tail. The tail phase is strongly

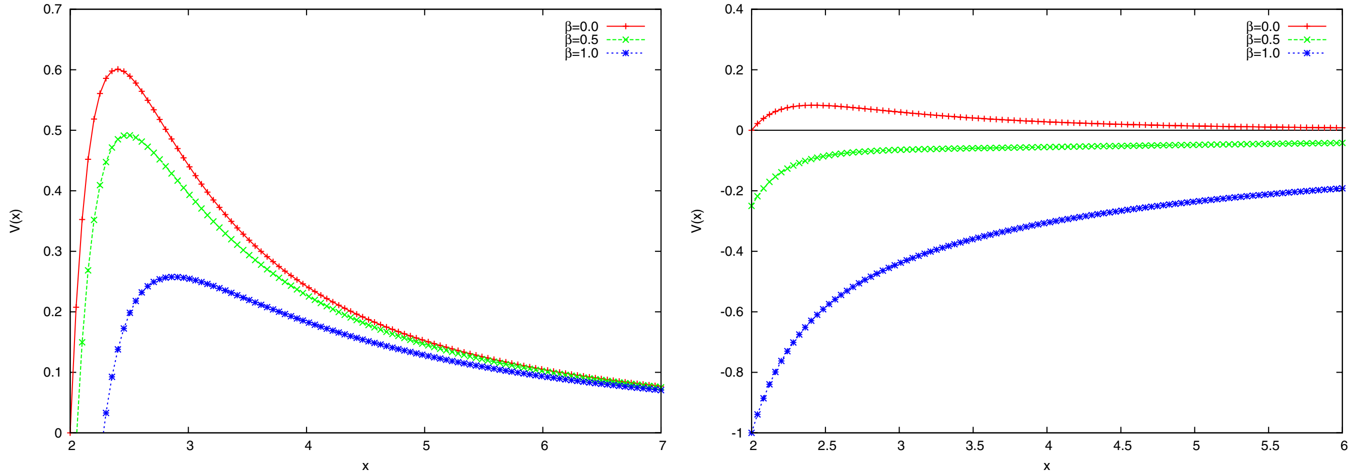

FIG. 1 (color online). Effective potential for several values of β. The p-brane parameters are $a = 2$, $b = 1$, $L = 1$; and $p = 3$ (left), $p = 6$ (right).

dependent on the value of the parameter β. For $\beta = 0$, we have a nonoscillatory power-law decay. But if $\beta \neq 0$, the tail is oscillatory, with a power-law envelope. Typical profiles are shown in Fig. 2.

Given the potential, we use the sixth order WKB technique [20] to obtain the quasinormal frequencies k. From the numerical data $Z_L(t, x_{\mathrm{fixed}})$, it is possible to estimate the fundamental quasinormal frequency with reasonable accuracy. Some results from both methods are given in Tables I, II, and III for $\beta = 0$. The concord between them is good. However, notice that for $p = 6$ and $L = 0$, our result should be taken with reservation. Higher overtones are not accessible by the "time-domain" technique. The corresponding WKB results are presented in Table III.

The dependence of the frequencies $\omega = \sqrt{k^2 + \beta^2}$ on β was also investigated. Both WKB and direct integration methods were employed, although the time evolution approach is not applicable for large β, since in this regime the massive tail dominates from a very early time. Nevertheless, it should be reliable for small β. Generally, we observed that for large values of the mass parameter, as β increases the frequencies becomes more oscillatory and less damped. One intriguing point was seen in a specific choice of parameters, namely $a = 2$, $b = 0.5$, $L = 0$, and

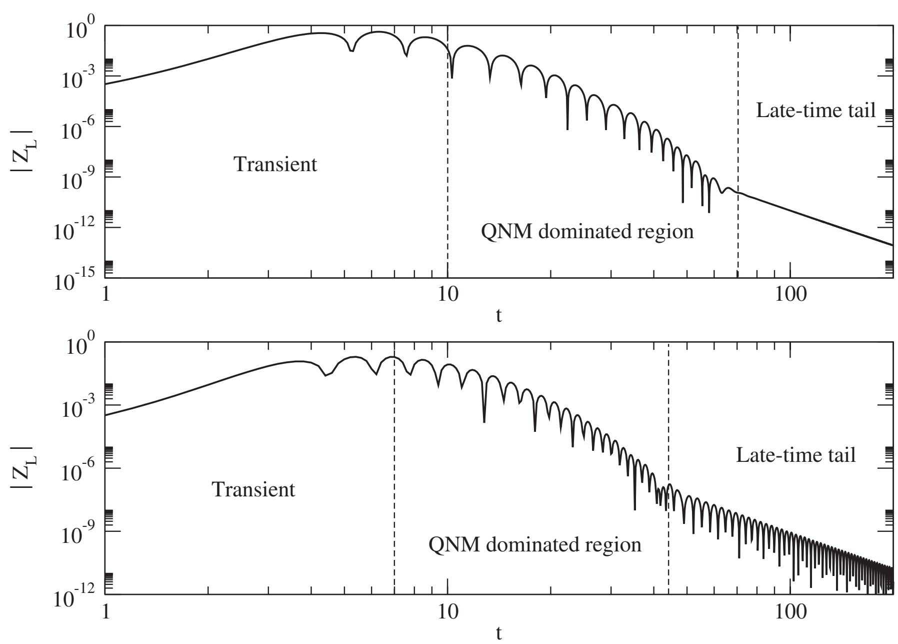

FIG. 2. Log-log graph of the absolute value of $Z_L(t, x_{\mathrm{fixed}})$. The quasinormal and tail phases are indicated. The p-brane parameters are $p = 0$, $a = 2$, $b = 0.5$, $L = 1$ and $\beta = 0$ (top), $\beta = 1$ (bottom).

TABLE I. Fundamental quasinormal frequencies with $a = 2$ and $b = 0.5$ for $p = 0, 1, 2, 3$.

	$p = 0$			
	WKB		Time evolution	
L	Re(k)	−Im(k)	Re(k)	−Im(k)
0	1.2889	0.5506	1.250 (3.0)	0.4980 (9.6)
1	1.5047	0.5876	1.606 (6.7)	0.4867 (17.2)
2	1.9638	0.4812	1.962 (0.092)	0.4805 (0.15)

	$p = 1$			
	WKB		Time evolution	
L	Re(k)	−Im(k)	Re(k)	−Im(k)
0	1.0812	0.4670	1.042 (3.6)	0.4498 (3.7)
1	1.3245	0.4963	1.604 (21.1)	0.463 (6.7)
2	1.7264	0.4301	1.725 (0.079)	0.4295 (0.13)

	$p = 2$			
	WKB		Time evolution	
L	Re(k)	−Im(k)	Re(k)	−Im(k)
0	0.8714	0.3911	0.8346 (4.2)	0.3926 (0.38)
1	1.1311	0.4137	1.161 (2.64)	0.3803 (8.1)
2	1.488	0.3754	1.488 (0.013)	0.3749 (0.13)

	$p = 3$			
	WKB		Time evolution	
L	Re(k)	−Im(k)	Re(k)	−Im(k)
0	0.6633	0.3202	0.6376 (3.9)	0.3279 (2.4)
1	0.9284	0.3363	0.9413 (1.4)	0.3204 (4.7)
2	1.2489	0.3162	1.249 (0.0056)	0.3157 (0.14)

$p = 2$. In this case, the WKB and time evolution methods give discrepant results near $\beta = 1$, as shown in Fig. 3.

It is worth noticing that the frequency k shows an almost scaling behavior on functions of a^{-1}, as shown in Fig. 4. That happens for the imaginary as well as for the real parts of k except for very small values of a. We found a different behavior just in the case $L = 2$, $n = 2$, for the values of $a < 2$ near the extremal case $a = b$. No instability has been found. For higher dimensions the real and imaginary parts of the frequency decrease. An exception is the case $L = 2$, $n = 2$: the real part of the frequency increases in the range $0 \leq p \leq 3$ and decreases for the others values of p, but the imaginary part decreases when p increases as for all others values of L and n that we considered in this work. We have found that, for a given value of L increasing the overtone number n, the frequencies become more damped, as we expected.

Although in general the calculation of the quasinormal frequencies can only be made using numerical methods, in the present scenario there is an important limit where an analytic expression is available. Expanding the effective potential in terms of small values of $1/L$ and using the WKB method in the lowest order (which is exact in this

TABLE II. Fundamental quasinormal frequencies with $a = 2$ and $b = 0.5$ for $p = 4, 5, 6$.

	$p = 4$			
	WKB		Time evolution	
L	Re(k)	−Im(k)	Re(k)	−Im(k)
0	0.4632	0.2514	0.4449 (4.0)	0.2555 (1.6)
1	0.7211	0.2607	0.7244 (0.46)	0.2438 (6.4)
2	1.0081	0.2512	1.008 (0.012)	0.2509 (0.13)

	$p = 5$			
	WKB		Time evolution	
L	Re(k)	−Im(k)	Re(k)	−Im(k)
0	0.2825	0.1828	0.2697 (4.5)	0.1990 (8.8)
1	0.5179	0.1843	0.5187 (0.16)	0.1828 (0.83)
2	0.7690	0.1804	0.7691 (0.010)	0.1802 (0.082)

	$p = 6$			
	WKB		Time evolution	
L	Re(k)	−Im(k)	Re(k)	−Im(k)
0	0.3135	0.05970	0.1485 (52.6)	0.1290 (116.1)
1	0.3608	0.1154	0.3616 (0.22)	0.1150 (0.34)
2	0.5890	0.1135	0.5889 (0.021)	0.1134 (0.042)

TABLE III. High overtone quasinormal frequencies with $a = 2$ and $b = 0.5$.

		$p = 0$		$p = 1$	
L	n	Re(k)	−Im(k)	Re(k)	−Im(k)
1	1	0.985 828	1.799 11	0.892 835	1.582 05
2	1	1.470 92	1.617 06	1.3581	1.390 48
2	2	0.408 755	2.806 27	0.538 849	2.555 82

		$p = 2$		$p = 3$	
L	n	Re(k)	−Im(k)	Re(k)	−Im(k)
1	1	0.798 307	1.340 85	0.693 083	1.092 24
2	1	1.222 35	1.188 43	1.0673	0.990 437
2	2	0.638 727	2.209 14	0.690 423	1.820 98

		$p = 4$		$p = 5$	
L	n	Re(k)	−Im(k)	Re(k)	−Im(k)
1	1	0.572 698	0.841 449	0.439 874	0.587 662
2	1	0.895 481	0.781 983	0.710 916	0.557 03
2	2	0.681 196	1.409 16	0.609 848	0.980 543

		$p = 6$	
L	n	Re(k)	−Im(k)
1	1	0.325 148	0.365 934
2	1	0.568 875	0.345 275
2	2	0.537 292	0.587 244

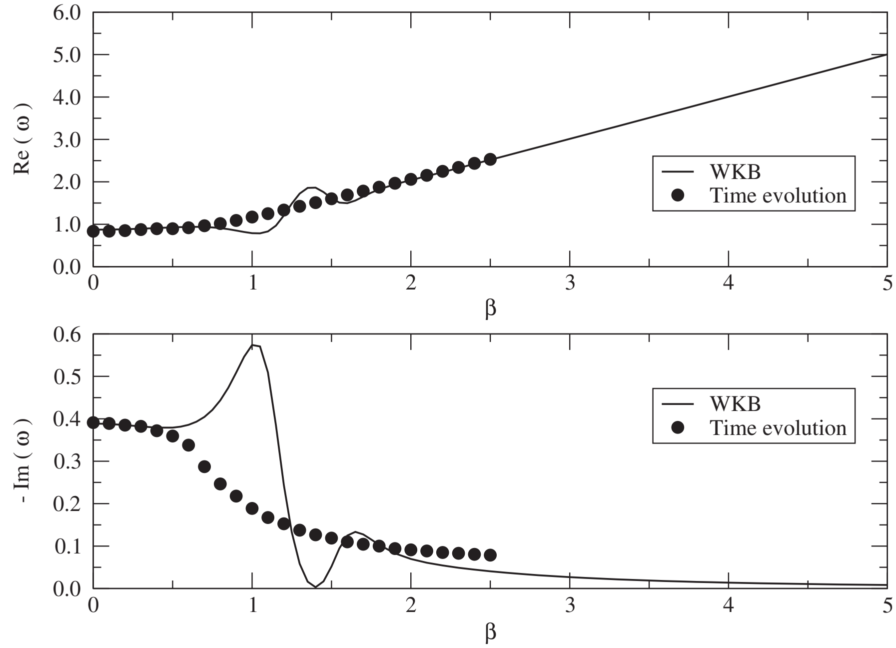

FIG. 3. Effect of β on the behavior of ω for $p = 2$ with $a = 2$, $b = 1$, and $L = 0$. Two different numerical methods were employed. They are consistent for small and large enough β, but discrepant near $\beta = 1$.

limit), we obtain

$$\omega^2 = L^2\Gamma(x_m) - i\left(n + \frac{1}{2}\right)L\Lambda(x_m), \tag{14}$$

where $\Gamma(x) = \frac{A(x)}{x^2 D(x)}$, $\Lambda(x) = -\frac{2A(x)}{C(x)} \times \sqrt{\frac{\Gamma(x)'}{2}[\ln(A(x)/C(x))]' + \Gamma''}$. The peak of effective potential is determined by $V(x)'$, and occurs at $x_m = [-2c_1/(c_2 + (c_2^2 - 8c_1)^{1/2})]^{1/(7-p)}$, with $c_1 = (7-p)\times(ab)^{7-p}$ and $c_2 = -(9-p)a^{7-p}$.

Far from the horizon the effective potential (with $\beta = 0$), in terms of $r_\star$, assumes the form

$$V(r_\star) = \begin{cases} (L + \frac{8-p}{2})(L + \frac{6-p}{2})\frac{1}{r_\star^2} + \mathcal{O}(\frac{1}{r_\star^{8-p}}) & \text{if } 0 \le p < 6 \\ L(L+1)[\frac{1}{r_\star^3} + (2a - b)\frac{\ln r_\star}{r_\star^4}] + \mathcal{O}(\frac{\ln r_\star}{r_\star^5}) & \text{if } p = 6 \quad \text{and} \quad L = 0 \\ L(L+1)[\frac{1}{r_\star^2} + (2a - b)\frac{\ln r_\star}{r_\star^3}] + \mathcal{O}(\frac{\ln r_\star}{r_\star^4}) & \text{if } p = 6 \quad \text{and} \quad L > 0. \end{cases} \tag{15}$$

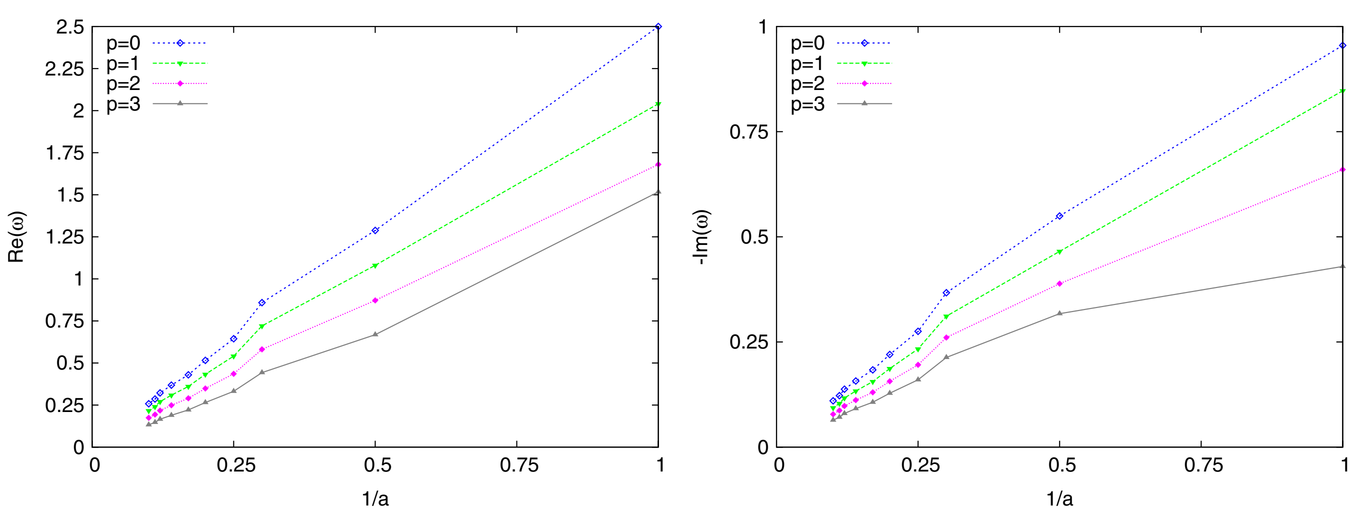

FIG. 4 (color online). Effect of the a parameter on quasinormal frequency. The p-brane parameters are $b = 0.5$, $L = 0$; and $\beta = 0$.

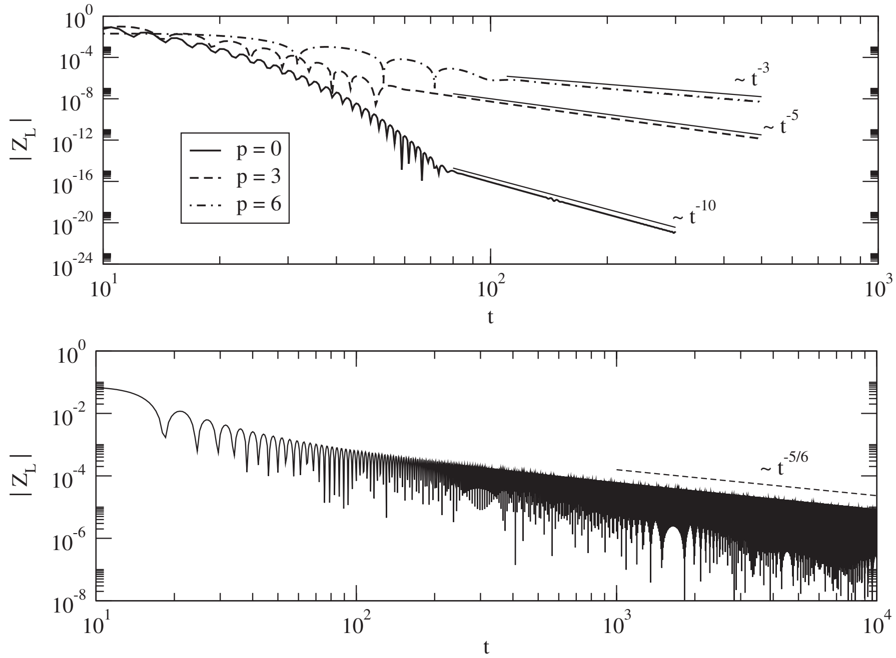

FIG. 5. (Top) Tails for several values of p. The power-law coefficients estimated from the numerical data (with $t > 250$) are: -10.01 ($p = 0$), -5.07 ($p = 3$), and -3.15 ($p = 6$). The analytical results (indicated by straight lines) are: -10 ($p = 0$), -5 ($p = 3$), and -3 ($p = 6$). The p-brane parameters are $a = 2$, $b = 0.5$, $L = 0$, and $\beta = 0$. (Bottom) Massive tail for $p = 6$. The envelope power-law coefficient estimated from the numerical data (with $t > 9000$) is -0.84. The analytical result (indicated by a straight line) is $-5/6 \approx -0.833$. The p-brane parameters are $a = 2$, $b = 0.5$, $L = 0$, and $\beta = 1$.

With this effective potential, it is shown [26,27] that initial data with compact support evolves, at late time, according to

$$\Psi_L \sim t^{-\alpha(p,L)}. \tag{16}$$

Therefore, at asymptotically late times the massless perturbation decays as a power-law tail.

The power-law coefficient $\alpha(p, L)$ reflects the potential asymptotic behavior. For $p = 1, 3, 5, 6$, $\alpha(p, L)$ can be analytically determined using the results in [27]:

$$\alpha(p, L) = \begin{cases} 2L - p + 8 & \text{with } p = 1, 3, 5 \\ 2L + 3 & \text{with } p = 6. \end{cases} \tag{17}$$

For $p = 0, 2, 4$, our numerical results suggest a similar expression

$$\alpha(p, L) = 2L - p + 10 \quad \text{with} \quad p = 0, 2, 4. \tag{18}$$

The tails are confirmed by the time-dependent approach. We illustrate these results in Fig. 5.

In the massive case, the asymptotic form of the effective potential changes. For large $r_\star$ we have

$$V(r_\star) = \begin{cases} \beta^2 + (L + \frac{8-p}{2})(L + \frac{6-p}{2})\frac{1}{r_\star^2} + \mathcal{O}(\frac{1}{r_\star^{8-p}}) & \text{if } 0 \le p < 5 \\ \beta^2 + [\beta^2 + L^2 + 2L + \frac{3}{4}]\frac{1}{r_\star^2} + \mathcal{O}(\frac{1}{r_\star^3}) & \text{if } p = 5 \\ \beta^2(1 + \frac{b-a}{r_\star}) + \mathcal{O}(\frac{1}{r_\star^3}) & \text{if } p = 6 \quad \text{and} \quad L = 0 \\ \beta^2(1 + \frac{b-a}{r_\star}) + [\beta^2 b(b-a) + L(L+1)]\frac{1}{r_\star^2} + \mathcal{O}(\frac{\ln r_\star}{r_\star^3}) & \text{if } p = 6 \quad \text{and} \quad L > 0\xi. \end{cases} \tag{19}$$

We have observed from the numerical simulations that the late-time tail has the form

$$\Psi_L \sim \sin(\beta t) t^{-\gamma(p,L)}. \tag{20}$$

If $p = 6$, the results in [28–30] apply, and the coefficient in the power-law envelope can be determined analytically: $\gamma(p = 6, L) = 5/6$. This result is illustrated in Fig. 5. For other values of p the analytical problem remains open.

V. EXTREME CASE

The analysis of the extreme case geometry is more subtle. If $p = 3$, we have a black-hole solution and the

TABLE IV. Scalar quasinormal frequencies for the extreme case ($a = b = 1$).

		$p = 0$		$p = 1$	
L	n	Re(k)	−Im(k)	Re(k)	−Im(k)
0	0	2.499 71	0.955 112	2.040 71	0.847 233
1	0	3.070 66	1.017 71	2.689 02	0.863 596
1	1	2.413 19	2.083 26	1.9794	2.175 09
2	0	3.886 48	0.931 587	3.475 84	0.802 949
2	1	3.159 79	2.7734	2.882 55	2.406 14
2	2	0.087 680 8	2.4072	0.978 905	3.541 21

		$p = 2$		$p = 3$	
L	n	Re(k)	−Im(k)	Re(k)	−Im(k)
0	0	1.6804	0.659 786	1.516 62	0.429 531
1	0	2.356 16	0.685 455	2.092 21	0.522 615
1	1	1.798 34	1.903 49	1.7917	1.466 52
2	0	3.105 46	0.658 724	2.798 37	0.513 388
2	1	2.678 48	1.977 19	2.525 34	1.558 01
2	2	1.520 44	3.229 54	1.927 28	2.572 06

		$p = 4$	
L	n	Re(k)	−Im(k)
0	0	1.400 21	0.323 76
1	0	2.008 24	0.340 953
1	1	1.829 87	0.991 697
2	0	13.399 173	15.362 158
2	1	2.524 47	1.050 96
2	2	2.195 58	1.732 77

problem is clearly formulated. If $p = 6$, we have a naked timelike singularity and the Cauchy problem is not well-posed (without additional conditions at the singularity). This class of solution will not be treated in the present work.

The novelty is the geometry with a null singularity. As discussed before, we have a well-posed initial value problem. We propose here to *define* the quasinormal modes in the same way they were defined in the black-hole scenario. This definition will be justified considering the wave problem in the following.

The effective potential for the scalar field perturbation in the extreme case scenario is obtained by taking $a = b$ in (12). This potential looks similar to the nonextreme case analog, and in terms of the tortoise coordinate, it tends to zero as $r_\star \to -\infty$ and $r_\star \to \infty$, which implies that the effective one-dimensional wave problem is similar to the previous nonextreme case. A bounded perturbation will therefore decay in time, which justifies the quasinormal mode definition adopted. As a side remark, we observe that for $p = 6$ the potential diverges near the horizon, a consequence of the timelike nature of the singularity at $r = a$. We have computed the quasinormal frequencies for $p < 5$. The results are shown in Table IV. We have sensible differences, by factors of order three.

For $L = 2$, from $n = 0$ to $n = 1$ we observe an increase in the decay rate. We found that the imaginary part increases, in the case $p = 0$ from $L = 2$, $n = 2$ to $n = 1$, in contrast with the behavior found in the nonextreme case. Otherwise, results are very similar to the nonextreme case.

VI. FINAL REMARKS

We studied the scalar perturbations of the full black p-brane solutions of ten-dimensional type IIB supergravity. The near the horizon limit of extremal p-branes is an $\mathrm{AdS}_{(p+2)} \times S^{(8-p)}$ space-time, which is dual to a $(p+1)$-dimensional conformal field theory at zero temperature. If we have an event horizon, the near horizon limit is a $(p+2)$-dimensional AdS black hole times a sphere $S^{(8-p)}$, dual to a field theory at finite temperature in $(p+1)$ dimensions. We obtained the same quasinormal spectrum using the standard procedure of considering a probe scalar field in the background geometry with a gauge-invariant formalism. The quasinormal mode structure in such a complex problem is amazingly simple. Allowing for a nonvanishing separation constant, later related to the glueball mass, the result is also very simple, displaying an almost scaling behavior. The tensor and scalar modes are exactly the same, leading to a simplicity of the results as well. Implications for the quark gluon plasma using the AdS/CFT relation awaits further analysis.

ACKNOWLEDGMENTS

This work has been supported by FAPESP and CNPq, Brazil, as well as ICTP, Trieste.

[1] J. Polchinski, *String Theoy* (Cambridge University Press, Cambridge, England, 1998), Vols. I, II; B. Zwiebach, *A First Course in String Theory* (Cambridge University Press, Cambridge, England, 2004).
[2] J. Maldacena, Adv. Theor. Math. Phys. **2**, 231 (1998).
[3] O. Aharony, S. Gubser, J. Maldacena, H. Ooguri, and Y. Oz, Phys. Rep. **323**, 183 (2000).
[4] G. W. Gibbons and P. K. Townsend, Phys. Rev. Lett. **71**, 3754 (1993).
[5] E. Shuryak, Prog. Part. Nucl. Phys. **53**, 273 (2004); S. Gubser, Gen. Relativ. Gravit. **39**, 1533 (2007); S. Gubser, Phys. Rev. D **74**, 126005 (2006); J. Friess *et al.*, J. High

Energy Phys. 04 (**2007**) 080.

[6] G. Policastro, D. T. Son, and A. O. Starinets, J. High Energy Phys. 09 (2002) 043; D. T. Son and A. O. Starinets, J. High Energy Phys. 09 (2002) 042; Annu. Rev. Nucl. Part. Sci. **57**, 95 (2007); J. High Energy Phys. 03 (2006) 052.

[7] P. Kotvun, D. T. Son, and A. O. Starinets, Phys. Rev. Lett. **94**, 111601 (2005); P. Kotvun, D. T. Son, and A. O. Starinets, J. High Energy Phys. 10 (2003) 064; A. O. Starinets, Phys. Rev. D **66**, 124013 (2002).

[8] C. Csaki, H. Ooguri, Y. Oz, and J. Terning, J. High Energy Phys. 01 (1999) 017.

[9] H. Boschi-Filho and N. R. F. Braga, J. High Energy Phys. 05 (2003) 009.

[10] A. S. Miranda, C. A. Ballon Bayona, H. Boschi-Filho, and N. R. F. Braga, J. High Energy Phys. 11 (2009) 119.

[11] S. Chandrasekhar, *The Mathematical Theory of Black Holes* (Oxford University, New York, 1983).

[12] H. Kodama and A. Ishibashi, Prog. Theor. Phys. **110**, 701 (2003); H. Kodama, A. Ishibashi, and O. Seto, Phys. Rev. D **62**, 064022 (2000).

[13] K. D. Kokkotas and D. G. Schmidt, Living Rev. Relativity **2**, 2 (1999); E. W. Leaver, Phys. Rev. D **45**, 4713 (1992); C. Gundlach, R. H. Price, and J. Pullin, Phys. Rev. D **49**, 883 (1994); E. Abdalla, R. A. Konoplya, and C. Molina, Phys. Rev. D **72**, 084006 (2005).

[14] V. Cardoso and J. P. S. Lemos, Phys. Rev. D **67**, 084020 (2003); R. A. Konoplya and A. Zhidenko, J. High Energy Phys. 06 (2004) 037; R. A. Konoplya, Phys. Rev. D **68**, 124017 (2003).

[15] B. Wang, C. Y. Lin, and E. Abdalla, Phys. Lett. B **481**, 79 (2000); B. Wang, E. Abdalla, and C. Molina, Phys. Rev. D **63**, 084001 (2001); C. Molina, D. Giugno, E. Abdalla, and A. Saa, Phys. Rev. D **69**, 104013 (2004); E. Abdalla, B. Cuadros Melgar, C. Molina, and A. Pavan, Nucl. Phys. **B752**, 40 (2006).

[16] Jaqueline Morgan, Vitor Cardoso, Alex S. Miranda, C. Molina, and Vilson T. Zanchin, J. High Energy Phys. 09 (2009) 117.

[17] G. T. Horowitz and A. Strominger, Nucl. Phys. **B360**, 197 (1991).

[18] A. Erdelyi, *Higher Transcendental Functions* (McGraw-Hill, New York, 1953), Vol. 2, pg. 232.

[19] Hans-Peter Nollert and Bernd G. Schmidt, Phys. Rev. D **45**, 2617 (1992).

[20] R. A. Konoplya, Phys. Rev. D **68**, 024018 (2003).

[21] C. Gundlach, R. Price, and J. Pullin, Phys. Rev. D **49**, 883 (1994).

[22] P. R. Brady, C. M. Chambers, W. Krivan, and P. Laguna, Phys. Rev. D **55**, 7538 (1997).

[23] C. Molina, D. Giugno, E. Abdalla, and A. Saa, Phys. Rev. D **69**, 104013 (2004).

[24] R. A. Konoplya and A. Zhidenko, Nucl. Phys. **B777**, 182 (2007).

[25] R. A. Konoplya and A. Zhidenko, Phys. Rev. D **78**, 104017 (2008).

[26] R. H. Price, Phys. Rev. D **5**, 2419 (1972).

[27] E. S. C. Ching, P. T. Leung, W. M. Suen, and K. Young, Phys. Rev. D **52**, 2118 (1995).

[28] H. Koyama and A. Tomimatsu, Phys. Rev. D **65**, 084031 (2002).

[29] H. Koyama and A. Tomimatsu, Phys. Rev. D **64**, 044014 (2001).

[30] R. A. Konoplya, A. Zhidenko, and C. Molina, Phys. Rev. D **75**, 084004 (2007).